Marine Energy Research

SCIEPublish

Article

A Conceptual Probabilistic Framework for Site-Specific Renewable-Energy Infrastructure Selection in Offshore Aquaculture

Thomas Vickers [1] and Damon Howe [1,2,*]

[1] Centre for Maritime Engineering and Hydrodynamics, Australian Maritime College, University of Tasmania, Locked Bag 1395, Launceston, TAS 7250, Australia; thomas.vickers@utas.edu.au (T.V.)

[2] Blue Economy Cooperative Research Centre, Launceston, TAS 7250, Australia

* Corresponding author. E-mail: damon.howe@utas.edu.au (D.H.)

Received: 3 August 2026; Revised: 3 September 2026; Accepted: 16 September 2026; Available online: 28 September 2026

ABSTRACT: Offshore expansion of aquaculture is constrained by the prohibitive cost of subsea grid connection, making off-grid renewable generation an alternative to the diesel supply that currently dominates. This study addresses a fundamental question: is there an optimal renewable energy infrastructure suitable for universal deployment in offshore aquaculture, or must solutions be site-specific? A probabilistic decision-making framework incorporating influence diagrams, Markov chains, temporal modelling, investment cost forecasting, and five renewable energy infrastructure designs was evaluated against performance, environmental impact, and techno-economic criteria. Application to two Tasmanian case study sites revealed that multi-source renewable infrastructures outperformed single-source alternatives, yet different technology combinations proved optimal at each location (VAWT-PV-OWC at Bass Strait, HAWT-PV or HAWT at Storm Bay). Under equal criterion weighting, renewable alternatives scored 15–35% lower in utility than diesel generation, at a cost of valued energy approximately 9–14 times the diesel baseline on a 2030 forecast basis, but this ranking reversed once environmental weighting exceeded 37%, within the range of plausible stakeholder priorities. The site-specific rankings were unchanged across all 64 cost-parameter perturbation scenarios tested, indicating robustness to cost-forecast uncertainty. These findings demonstrate that effective renewable energy deployment for offshore aquaculture requires site-specific assessment rather than a one-size-fits-all approach, and provide a transferable methodology for conducting assessment.

Keywords: Hybrid renewable energy systems; Discrete-time Markov chain; Multi-criteria decision making; Cost of valued energy; Multi-attribute utility theory; Off-grid power supply; Offshore aquaculture

1. Introduction

Global aquaculture market values exceeded $41 billion USD in 2023, with a forecast compound annual growth of 8.2% [1], driving a transition from nearshore to offshore environments as coastal zone limitations become more pronounced, including reduced user conflicts, disease mitigation, and lessened ecological impact [2–4]. In Tasmania, where Atlantic salmon farming constitutes a $1 billion AUD annual industry

© 2026 The authors. This is an open access article under the Creative Commons Attribution 4.0 International License (https://creativecommons.org/licenses/by/4.0/).

[5], government initiatives such as the Tasmanian Salmon Industry Plan [6] actively promote offshore expansion through investment certainty and innovation partnerships. However, this transition confronts a critical technological gap: offshore sites (>2 km from coast) [7] face prohibitive grid connection costs—exceeding $3.8 million AUD for 2 km subsea cables [8]—while requiring survivable infrastructure capable of withstanding harsh marine conditions. Diesel generation, though reliable, presents unacceptable environmental impacts through greenhouse gas emissions and operational challenges, including frequent refueling [9], creating a fundamental dilemma: offshore aquaculture expansion requires power systems that are simultaneously reliable, environmentally sustainable, and economically viable.

Offshore renewable energy technologies offer potential solutions to this challenge, yet integration faces technical and practical barriers across the available options. Wind energy is the most commercialised, with horizontal axis wind turbines (HAWTs) scaled to 15 MW for grid applications [10], while emerging vertical axis wind turbines (VAWTs) offer advantages in turbulent conditions, omnidirectional operation, and compact footprints suited to small-scale arrays [11,12]. Floating photovoltaic (FPV) systems extend solar technology offshore with scalable, predictable generation beneficial for aquaculture operations, with pontoon-type foundations emerging as the most viable commercialisation pathway [13]. Wave energy converters (WECs), particularly oscillating water columns (OWCs), remain less mature than wind and solar [14] but offer modularity advantages for integration onto larger structures [15,16]. Resource intermittency across all three necessitates battery energy storage system (BESS) and backup diesel generation for supply security; multi-source platforms combining VAWTs, OWCs, and Photovoltaic (PV) can substantially reduce diesel dependency [17], though economic viability remains uncertain. Recent reviews confirm the continuing convergence of these two domains [18,19], including techno-economic analyses of wave energy co-located with aquaculture [20] and hybrid floating solar–wind systems [21].

Structured multi-criteria decision-making has also been extended recently to adjacent offshore renewable-energy problems: Bayesian-network-informed site selection for wave energy converters [22], investment appraisal of a floating wind–solar–aquaculture platform under a probabilistic linguistic environment [23], AHP–entropy–TOPSIS evaluation of offshore wind–fishery integration benefits [24], and expert-weighted concept selection for hybrid wave–current energy systems [25]. Table 1 situates the present framework relative to these and other closely related studies across seven dimensions: application domain; whether multiple renewable technologies are evaluated jointly (*Multi-tech*); whether uncertainty is treated probabilistically rather than deterministically (*Prob. Unc.*); whether storage is modelled as an explicit decision variable (*Storage*); whether the economic metric goes beyond plain Levelised Cost of Electricity (LCOE) (*Econ. >LCOE*); the core decision-making Method; and whether the ranking is checked against empirical or operational case data rather than only an internal consistency check (*Valid.*).

This technological landscape reveals a critical knowledge gap: while individual renewable technologies show promise, no systematic framework exists to evaluate alternative configurations that account for site-specific resource uncertainty, multiple competing decision criteria, and the stochastic nature of marine resources. Current practice offers no clear guidance on whether single-source systems (e.g., large offshore HAWTs) or multi-source approaches are superior, nor whether a universally deployable solution exists or site-specific configurations are required.

Table 1. Comparative classification of the present framework against closely related offshore renewable-energy decision-support studies. ✓ = criterion met; × = criterion not met.

Study	Domain	Multi-Tech	Prob. Unc.	Storage	Econ. >LCOE	Method	Valid.
Present study	Aquaculture power supply	✓	✓	✓	✓	ID + DTMC + AHP/MAU	×
Roberts et al. [17]	Aquaculture power supply	✓	×	×	×	Deterministic time-series	✓

Villalba et al. [7]	Co-located aquaculture/wind	×	✓	×	×	Bayesian network/ID	✓
Vanegas-Cantarero et al. [26]	Offshore renewables (general)	×	×	×	✓	Conceptual MCDM	×
Abaei et al. [27]	Marine renewable energy	×	✓	×	×	Risk-based MCDM	✓
Salvador et al. [28]	Offshore wind siting	×	×	×	×	Deterministic MCDM	✓
Bao et al. [22]	WEC site selection	×	✓	×	×	Bayesian network + MCDM	✓
Mao et al. [23]	Wind-solar-aquaculture invest.	✓	✓ †	×	✓	PLTS + DEMATEL + entropy	×
Fang et al. [24]	Wind-fishery integration	×	×	×	✓	AHP + entropy + TOPSIS	✓
Ng and Ong [25]	Hybrid WEC-HKT selection	✓	×	×	×	MCDA (SAW) + expert wt.	×

† Uncertainty treated via expert-elicited/linguistic scoring rather than temporal resource stochasticity.

Traditional techno-economic evaluation methods inadequately address this decision environment. Multi-criteria decision making (MCDM) provides systematic frameworks for evaluating alternatives across conflicting objectives [29], with techniques including Analytical Hierarchy Process (AHP), Multi-Attribute Utility Theory (MAUT), and Technique for Order of Preference by Similarity to Ideal Solution (TOPSIS) widely applied in energy system assessment; however, conventional MCDM approaches evaluate decisions under certainty, assuming known consequences and deterministic attributes. The LCOE, though standard for grid-connected renewables, poorly captures off-grid advantages and disadvantages [26], failing to account for generation–demand mismatches where excess Power has zero value. More critically, traditional techno-economic methods cannot accommodate the stochastic behaviour of wind, solar, and wave resources in marine environments. This creates a second gap: existing frameworks have yet to assess how resource variability propagates through system performance, environmental impact, and economic outcomes, thereby influencing infrastructure selection. Influence diagrams have been applied to offshore renewable energy site selection [7,27,28], but their integration with probabilistic temporal modelling for infrastructure evaluation in aquaculture contexts remains unexplored.

Roberts et al. [17] established the multi-source offshore aquaculture platform concept and the demand-profile methodology adopted here, and evaluated performance deterministically. The present study advances this foundation via a probabilistic decision-making framework integrating a Bayesian influence diagram [30] with discrete-time Markov chain (DTMC) temporal modelling [31], applied by (i) quantifying resource intermittency probabilistically through DTMC modelling rather than deterministic time-series comparison; (ii) propagating these probabilities through the influence-diagram framework to compute multi-criteria expected utilities across performance, environmental, and economic criteria, with weights informed by the AHP [32], rather than reporting performance metrics in isolation; and (iii) systematically ranking single- and multi-source configurations against a diesel baseline across two contrasting sites, directly testing whether a universally optimal configuration exists.

The research addresses three questions: (1) Can renewable energy infrastructures achieve utilities comparable to diesel generation across technical performance, environmental impact, and economic feasibility criteria? (2) Do optimal renewable configurations differ across sites with varying resource characteristics, or does a universally deployable solution exist? (3) How do stakeholder priorities, expressed through multi-attribute utility weightings, influence infrastructure rankings and the competitiveness of renewable versus diesel alternatives? In answering these questions, this work contributes a transferable probabilistic decision-making framework for off-grid renewable energy evaluation under uncertainty, offering practical guidance for policymakers on economic incentives that align renewable costs with environmental objectives, and for offshore developers and aquaculture operators implementing systematic

infrastructure selection incorporating local resource data and stakeholder priorities. The paper is structured as follows: Section 2 outlines the theoretical foundations of the framework; Section 3 describes the methodology, including numerical model architecture; Section 4 details the case study for two Tasmanian sites; Section 5 presents results, discussion, and implications; and Section 6 provides conclusions on site-specific renewable energy deployment for offshore aquaculture.

2. Theory

To evaluate alternative solutions for powering offshore aquaculture using an influence diagram, the stochastic behaviour of renewable energy systems must be modelled through temporal power generation datasets compared against aquaculture demand profiles. Probabilistic techniques quantify uncertainties in power generation performance, environmental impact, and economic attributes. The numerical model integrates influence diagram frameworks with temporal modelling, applying utility theory to rank renewable energy solutions against conventional diesel generation. A case study demonstrates this decision-making structure through rudimentary sizing of single-source and multi-source renewable energy configurations.

2.1. Influence Diagram

An influence diagram extends Bayesian networks [30] by adding decision and value nodes to graphical representations of probabilistic dependencies among uncertain variables. Bayesian networks comprise of chance nodes (representing uncertain variables through probability distributions) and acyclic directional connections (representing influence direction). These networks determine probabilities of multiple random events occurring through Bayes' theorem:

$$\mathrm{P(A \mid B)} = \frac{\mathrm{P(B \mid A)P(A)}}{\mathrm{P(B)}} \tag{1}$$

where A and B are events with P(B) ≠ 0, P(A|B) represents conditional probability of A given B, P(B) is the prior probability, and P(A) is the posterior probability. For scenarios with multiple events:

$$\mathrm{P(A \mid B \cap C)} = \frac{\mathrm{P(B \mid A \cap C)P(A \mid C)}}{\mathrm{P(B \mid C)}} \tag{2}$$

where C represents a third event and B ∩ C indicates both events are true. Detailed Bayesian network theory is provided in [33]. Influence diagrams extend this framework through decision nodes (representing available alternatives) and value nodes (defining decision-maker preferences through rankings). The network calculates event likelihoods for each alternative and ranks them against value node preferences, maintaining acyclic structure.

2.2. Temporal Modelling

Probabilistic analysis of renewable energy infrastructures requires temporal event samples. Open-source datasets provide historical site-specific resources, including wind speeds, solar irradiation, significant wave height, and peak period at hourly intervals over annual cycles. These datasets were validated against regional meteorological observations to ensure representativeness. The MATLAB 2022a numerical model processes temporal resources into power generation time series following the methodology described in [17]. This implementation was modified to account for wind turbine hub height variations, applying the DNV-RP-C205 logarithmic wind profile relationship:

$$U(z) = \frac{u^*}{k_a} \ln \frac{z}{z_0} \tag{3}$$

where *U(z)* is wind speed at height z, k_a is von Karman's constant (0.4), z_0 is terrain roughness parameter (0.0001, representing worst-case ocean conditions), and:

$$u^* = \sqrt{\frac{k_a^2}{\left(\ln\frac{H}{Z_0}\right)^2}} \times U(10) \tag{4}$$

where H represents reference wind speed height (10 m). Temporal power generation feeds into influence diagrams to determine system surplus or deficit relative to demand.

2.3. Economic Analysis

Comparing economic characteristics requires consistent metrics. LCOE estimates the average construction and operating costs over the asset's lifetime, divided by the total power output [34]. While suitable for grid-connected systems where all electricity is sold at market prices, LCOE assumes an equivalent economic value for all generated Power—which is invalid for off-grid systems [35], where generation-demand mismatches render excess electricity valueless.

Cost of Valued Energy (COVE) [36] addresses this limitation by dividing annual costs by actual Power utilised rather than theoretical capacity. For off-grid aquaculture, this distinction proves critical: a system generating 1000 kWh but meeting only 600 kWh demand due to battery capacity constraints yields different economic assessments under LCOE (based on 1000 kWh) versus COVE (based on 600 kWh utilised). Since excess Power represents wasted energy when batteries reach capacity [35], COVE provides a realistic off-grid economic evaluation.

For off-grid applications, market electricity prices are irrelevant. Operational costs, which are difficult to predict for immature technologies, are assumed to be comparable across systems and thus neglected. The modified COVE metric is:

$$\text{COVE} = \frac{Annual\ Investment\ Cost}{Valued\ Energy} \tag{5}$$

expressed in \$/kWh, where valued energy represents renewable Power actually used by aquaculture operations annually. Investment cost forecasting [37] normalises technology maturity disparities through:

$$z = C_0^* x^a - \frac{b}{1 + e^{-c(y-d)}} + b \tag{6}$$

where z is the forecast annual investment cost (USD/kW), C_0^* is the current investment cost, x is accumulative installed capacity (GW), y is normalised technology readiness level (TRL) for the forecast year, and parameters a, b, c, d represent the learning rate, saturation value, ramp rate, and location value, respectively. Economic forecasting parameters were selected based on historical technology deployment data and validated against industry projections for 2030. Learning and ramp rates most significantly influence cost projections, reflecting technical progression and installation rates. For multi-source infrastructures, annual investment cost is the weighted average of individual technology costs proportional to rated capacity shares.

2.4. Probabilistic Analysis

Temporal power generation data feeds influence diagrams through probability distributions modelling stochastic processes. Renewable energy generation, dependent on resource availability, is modelled using Markovian approaches [31]. Markov chains describe probabilistic evolution of random quantities over time in memoryless systems where future states depend only on present states. DTMCs suit power generation time series analysis through hourly discretisation. State definitions align with aquaculture demand thresholds, selected based on operational requirements during salmon growth cycles to ensure physical relevance. This normalisation captures demand non-homogeneity across grow-out phases.

The influence diagram requires probability density functions from transition matrix stationary distributions. DTMCs count state transitions, with transition matrix Q:

$$Q = \begin{bmatrix} \lambda_{11} & \lambda_{12} & \cdots & \lambda_{1n} \\ \lambda_{21} & \lambda_{22} & & \lambda_{2n} \\ & \vdots & - & - \\ \lambda_{n1} & \lambda_{n2} & - & \lambda_{nn} \end{bmatrix} \tag{7}$$

where λ_{ij} represents the transition probability from state i to state j (e.g., λ_{n1} is the transition probability from state n to state 1), for $i,j \in \{1, \ldots, n\}$. Transition probabilities are calculated as state transition counts divided by total transitions in the time series. Stationary distributions, representing long-term probabilities of power generation within demand-defined states, are eigenvectors that satisfy DTMC requirements, with eigenvector sums equal to unity. Non-stochastic system qualities like cost employ deterministic probabilities (0 or 1) for given prior probabilities or decision node alternatives.

The DTMC formulation adopted here assumes time-homogeneous transition probabilities, *i.e.*, a single transition matrix estimated over the full annual dataset rather than separate matrices for distinct seasonal or diurnal regimes. This simplifying assumption was adopted because a single validated year of site-specific resource data was available for each case study site, which is insufficient to reliably estimate season-specific transition matrices without substantially increasing sampling variance in the less-populated seasonal subsets. Time-homogeneity is partially justified by the model structure itself: demand-state thresholds (Table 2) are defined on a monthly basis to reflect the salmon grow-out production cycle, so seasonal variation in *demand* is already captured at the influence-diagram level, and the DTMC is only required to represent the statistics of *generation* state transitions relative to those thresholds. Wind, solar, and wave resources nonetheless exhibit known diurnal and seasonal non-stationarity that a single annual transition matrix cannot fully resolve, and the reported stationary distributions should therefore be interpreted as long-run annual averages rather than season-specific operating probabilities. We identify seasonally-segmented or non-homogeneous Markov modelling, supported by multi-year resource datasets, as a priority methodological extension rather than a component of the present framework's current formulation.

Table 2. Aquaculture demand sets upper and lower thresholds based on a monthly profile of peaks and off-peaks, measured in kWh.

State	1	2	3	4	5	6	7	8
Lower Threshold	0	3	5	25	50	72.5	97.5	120
Upper Threshold	3	5	25	50	72.5	97.5	120	n/a

The fitted transition matrices were checked against the underlying data by comparing each infrastructure's theoretical stationary distribution against the empirical state-occupancy frequency observed directly in the temporal power generation series. Across all five infrastructures at both sites, the total variation distance between the theoretical and empirical distributions ranged from 0.0018 to 0.0033, indicating the fitted DTMC closely reproduces the data's long-run state-occupancy behaviour.

Within the influence diagram, a chance node can influence multiple posterior nodes. Where a marginal node's probability density function is computed by stochastic methods, it may carry the attributes of its prior probability. For example, the probability of a BESS being depleted, sufficiently charged, or overcharged depends on the surplus or deficit of the system. Applying Bayes' theorem, given in Equation (1), to solve for P(B) removes the prior probability from the Probability Density Function (PDF), expressed as:

$$\mathrm{P(B)} = \frac{\mathrm{P(B \mid A)P(A)}}{\mathrm{P(A \mid B)}} \tag{8}$$

where, in this application, A represents the surplus or deficit of generated Power relative to aquaculture demand, and B represents the resulting battery charge status (depleted, sufficiently charged, or overcharged); P(B) is thereby obtained without requiring the prior probability of A to be independently specified.

2.5. Utility Theory

Utility functions quantify decision-maker objectives and preferences in MCDM techniques, representing outcome preferences on 0–1 scales where 1 indicates maximum desirability [29]. Chance node outcomes are ranked against these preferences. Criteria are normalised through min-max scaling to ensure commensurability: each criterion's raw values are transformed to 0–1 scales before utility assignment, enabling consistent cross-criterion comparison.

For multiple objectives, MAUT uses multiple value nodes, each representing an individual objective. Additive linear utility (ALU) sums all utilities normalised against maximum possible utility (U_{MAX}). Multi-attribute utility (MAU) incorporates decision-maker weightings:

$$\mathrm{MAU} = \frac{W_1 \times U_1 + W_2 \times U_2 + \cdots + W_n \times U_n}{\mathrm{U_{MAX}}} \tag{9}$$

where W_i represents criterion i weight and U_i is the corresponding utility. The highest utility scores indicate the preferred alternatives for both approaches.

MAU assumes additive independence [38]—criterion preferences are independent of other criterion levels, which is reasonable for performance, environmental, and economic objectives. AHP [32] derives criterion weights through pairwise comparison judgement matrices using Saaty's 1–9 intensity scale. Principal eigenvectors, normalised to unity, yield weights. Consistency ratios below 0.1 validate judgement coherence [32], reducing cognitive biases inherent in direct weight assignment [39]. ALU and MAU outputs were cross-validated to ensure ranking consistency under equal weighting conditions, confirming computational accuracy.

This model primarily employs ALU with MAU sensitivity analysis exploring criterion weight variations on infrastructure rankings.

3. Methodology

A numerical model was developed in MATLAB 2022a following a structured four-phase architecture to evaluate renewable energy infrastructure alternatives for offshore aquaculture (Figure 1). The underlying MATLAB implementation—including resource data preprocessing, power conversion models for wind, solar, and wave resources, and hourly time-step handling for the temporal simulation—extends the numerical model of Roberts et al. [17], in which these components are described in full. The present study adds the probabilistic (DTMC and influence-diagram) and multi-criteria utility layers described in Sections 2.4 and 2.5 on top of this existing temporal simulation architecture.

3.1. Numerical Model Architecture

The *exploration phase* defines model inputs: infrastructure designs (rated capacities, platform dimensions, device configurations), site-specific resources (wind, solar, wave data from NASA Power Data Access Viewer and Geoscience Australia National Map, validated against regional Bureau of Meteorology observations for 2021), battery storage capacities (0–2000 kWh in 500 kWh increments), and aquaculture demand profiles representing Tasmanian Atlantic salmon production cycles adapted from [17].

The *technical analysis phase* processes these inputs through temporal power generation modelling at hourly resolution over annual cycles, investment cost forecasting using Equation (6) with parameters validated against industry projections for 2030 deployment, and COVE calculations via Equation (5). Utility functions are developed for each decision criterion via min-max normalisation, mapping outcomes to 0–1 preference scales, with boundary values representing the best and worst observed performances across all alternatives.

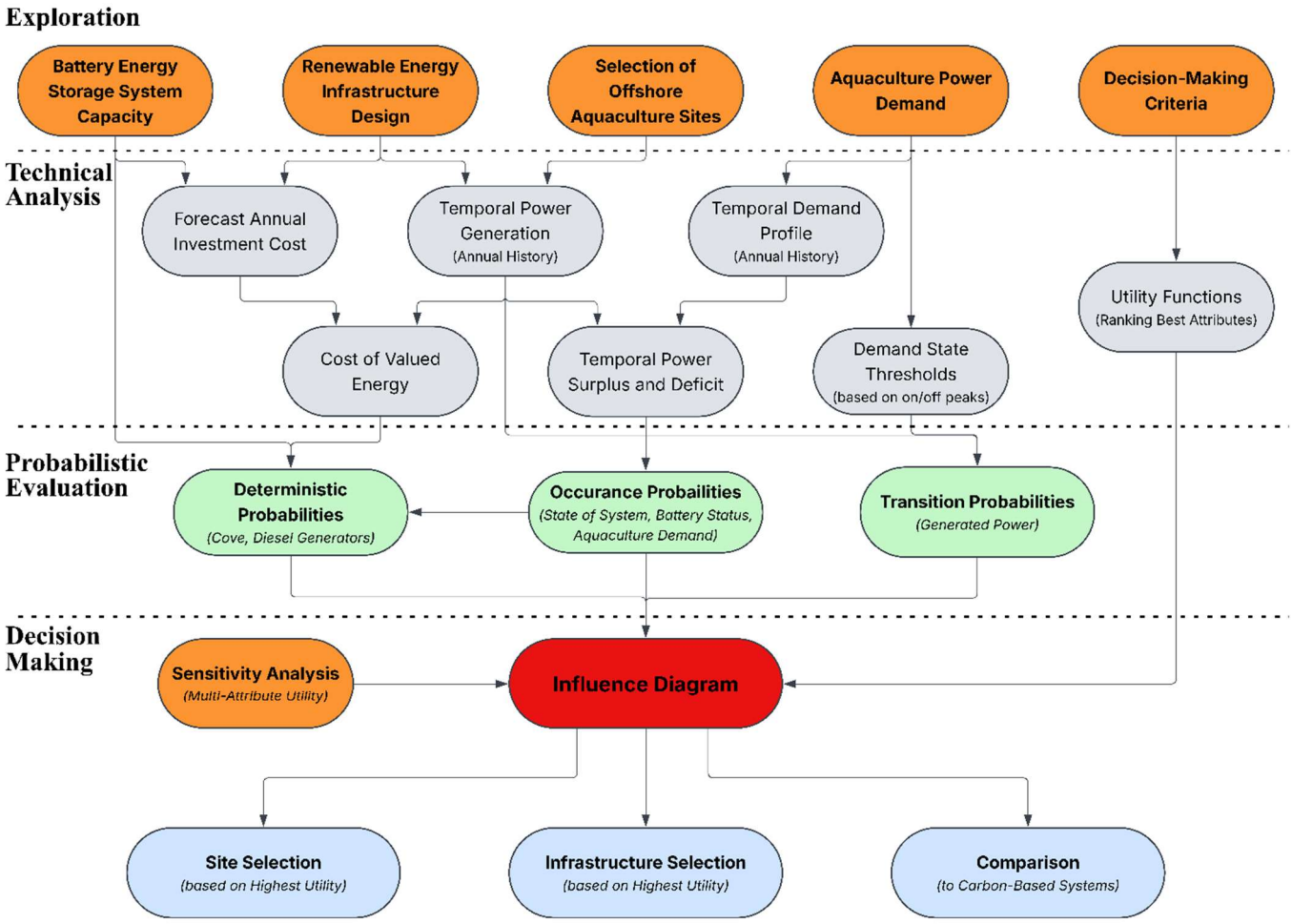


Figure 1. Methodology flow chart of the numerical model, showing the four phases of development: Exploration, Technical Analysis, Probabilistic Evaluation, and Decision Making. Arrows indicate workflow direction; cell colour denotes function—orange: model inputs, grey: technical analysis, green: probability distributions, blue: model outputs.

The *probabilistic evaluation phase* applies DTMC modelling to temporal power generation data, computing transition probability matrices and extracting stationary distributions through eigenvector analysis. Markov state boundaries align with aquaculture demand thresholds set by distinct operational phases of the salmon grow-out cycle—feeding intensity, lighting, ventilation, and pumping demand transitions (Table 2), establishing eight physically meaningful power states. Each threshold boundary corresponds to a documented operational transition rather than an evenly spaced partition of the demand range. Bayesian probability calculations determine battery status (depleted, charged, or overcharged) and state of system probabilities (sufficient or insufficient power) conditioned on infrastructure type, demand profile, and storage capacity. Interdependencies between generated Power, battery status, and diesel usage are quantified through conditional probability tables validated against 8750-h temporal simulations, ensuring consistency between stochastic modelling outputs and deterministic system constraints. These probability distributions populate influence diagram chance nodes.

The *decision-making phase* applies the influence diagram framework, in which Bayesian networks propagate probabilities from chance nodes through deterministic relationships to value nodes. Individual criterion utilities are calculated and aggregated through ALU (equal weighting) or MAU (Equation (9)) to rank alternatives. ALU and MAU computational consistency was verified by confirming identical rankings under equal MAU weights (0.333 each), validating the aggregation methodology. Sensitivity analysis explores how varying criterion weights affect infrastructure rankings under different stakeholder priorities.

3.2. Decision Criteria Selection

Three decision criteria evaluate alternative renewable energy infrastructures for offshore aquaculture: technical performance, environmental impact, and economic feasibility, aligning with established MCDM approaches for off-grid renewable energy systems [26,27,29].

Technical performance evaluates infrastructure reliability in meeting power demand, critical for aquaculture, where interruptions cause livestock mortality. This criterion is quantified through probability distributions of power states relative to demand thresholds and battery storage adequacy, with utility functions assigning maximum scores (1.0) when generation consistently meets or exceeds demand and minimum scores (0.0) for frequent deficits requiring diesel backup. Environmental impact assesses backup diesel generator usage as a carbon emissions proxy, addressing policy drivers motivating fossil fuel transition. Utility functions reward minimal diesel dependency, with maximum scores for zero diesel usage and scores decreasing linearly with diesel runtime. Economic feasibility captures investment cost normalised by valued energy delivered (COVE), representing the viability constraint for industry adoption. Economic utility assigns maximum scores to the lowest discretised COVE bin and decreases linearly across the discretised COVE range.

These criteria represent core pillars consistently identified across stakeholder priorities in isolated energy system planning [29], addressing aquaculture operator requirements (reliability, cost) and sustainability objectives (emissions reduction). While additional factors merit consideration (maintenance requirements, technology maturity, social acceptance, operational risk, and full lifecycle emissions beyond the operational diesel-usage proxy adopted here), these three provide the foundation for systematic infrastructure comparison and capture the primary trade-offs in off-grid renewable energy deployment.

3.3. Influence Diagram

A multi-attribute influence diagram was developed using open-source GeNIe Academic 5.0 software to evaluate offshore renewable energy systems for aquaculture (Figure 2). Decision nodes represent infrastructure alternatives and battery capacities, value nodes quantify criterion utilities, and chance nodes model uncertain system behaviours.

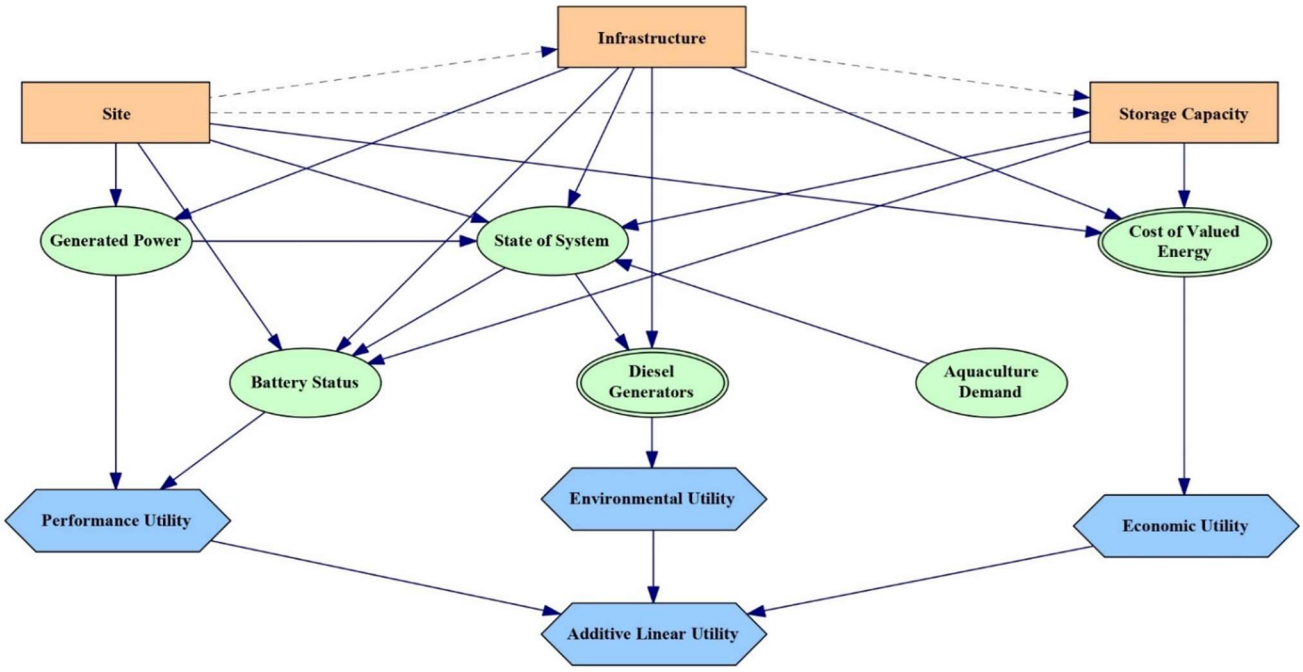


Figure 2. Developed an influence diagram framework for renewable energy systems in offshore aquaculture. Decision nodes are coloured orange, chance nodes are green, and value nodes are blue.

Probability propagation follows Bayesian network principles, with two distinct classes of chance nodes populated from the temporal simulation. Stochastic chance nodes (Generated Power, Battery Status) are populated directly from the DTMC stationary distributions and battery state-update outcomes described in Sections 2.4 and below; deterministic chance nodes (COVE, Diesel Generators) are populated via conditional probability tables with binary (0 or 1) outcomes fully determined by parent-node states, reflecting the physical logic that diesel backup activates if and only if the State of System is insufficient, and that COVE follows directly from the investment cost and valued energy already computed for each alternative. Value nodes then map these chance node outcomes to 0–1 utility scores via the criterion-specific utility functions defined in Section 2.5, with expected utility computed by summing the product of each outcome's probability and corresponding utility across all states Equation (9) yielding a single utility score for each alternative.

Performance utility depends on the Generated Power and Battery Status chance nodes. Generated Power employs Markovian stationary distributions from temporal power generation. Battery Status probability represents BESS states (depleted, charged, overcharged) at any time. The State of System chance node captures system surplus/deficit through Bernoulli distributions (sufficient or insufficient Power) as functions of demand and generation (Figure 3).

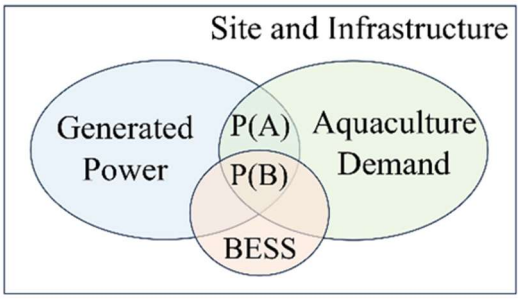


Figure 3. Venn Diagram illustrating the influence diagram probabilistic analysis relationships.

In Figure 3, P(A) represents the State of System probability relating generated Power to demand, while P(B) represents Battery Status dependency on P(A) and BESS capacity. Deterministic probability that Battery Status is depleted when the State of System is insufficient simplifies computation of charged or overcharged states given sufficient Power. Battery state of charge is tracked over the temporal simulation with an initial condition of 50% of the selected storage capacity. At each hourly time step, surplus generation (relative to demand) charges the battery up to its selected capacity limit (excess beyond maximum charge is treated as dissipated rather than utilised (Excess electricity beyond BESS capacity may in principle power auxiliary aquaculture operations such as desalination, amenities, pumping, or cleaning; as these fall outside the present research scope, this excess is treated as dissipated)). Conversely, generation deficits are met first from available battery charge, with any remaining shortfall met by backup diesel generation. This charge/discharge behaviour determines the Battery Status chance node outcomes (depleted, charged, overcharged) that feed the influence diagram. Reliability thresholds defining "sufficient power" were established at 95% demand satisfaction based on aquaculture industry standards for critical infrastructure, balancing operational security against renewable intermittency acceptance. The State of System node provides prior probability for the Diesel Generators chance node, representing backup generator usage probability when Power is insufficient through deterministic conditional tables (diesel used for insufficient Power, not used for sufficient Power). The COVE chance node represents valued energy cost for each infrastructure alternative, discretised into 20 states ranging \$0–40/kWh in \$2/kWh intervals, with discretisation resolution selected to balance computational efficiency against economic differentiation among alternatives.

The probabilities entering the influence diagram are therefore derived entirely from the temporal simulation, without expert elicitation or subjective assignment. The derivation proceeds in four steps: hourly generation for each infrastructure is classified into the eight demand-referenced states of Table 2; transitions between consecutive hourly states are counted to populate the transition matrix Q (Equation (7)), whose stationary distribution gives the long-run probability of generation occupying each state; battery status and state-of-system probabilities are obtained from the same time history by Bayesian conditioning (Equation (8)); and these probabilities are combined with the criterion utility functions through Equation (9) to give the expected utility of each alternative. The transition matrix and stationary distribution obtained for the multi-source infrastructure at Bass Strait are reported as a worked instance in the results. The fidelity of this representation against the underlying data is reported earlier in the theoretical development, and Appendix A sets out the full computational sequence.

The complete influence diagram, including all conditional probability tables, utility functions, and state definitions, is provided as Supplementary Material (GeNIe network file), enabling independent inspection and reproduction of the reported expected utility calculations.

4. Case Study

A case study for a theoretical offshore aquaculture installation showcases the decision-making framework's application and assesses alternative infrastructures. Key factors governing probabilistic analysis and influence diagram implementation include site characteristics, power demand, renewable energy infrastructure configurations, and energy storage systems. Two Tasmanian sites with contrasting resource profiles enable a comparative evaluation of how site-specific conditions influence optimal infrastructure selection (Figure 4).

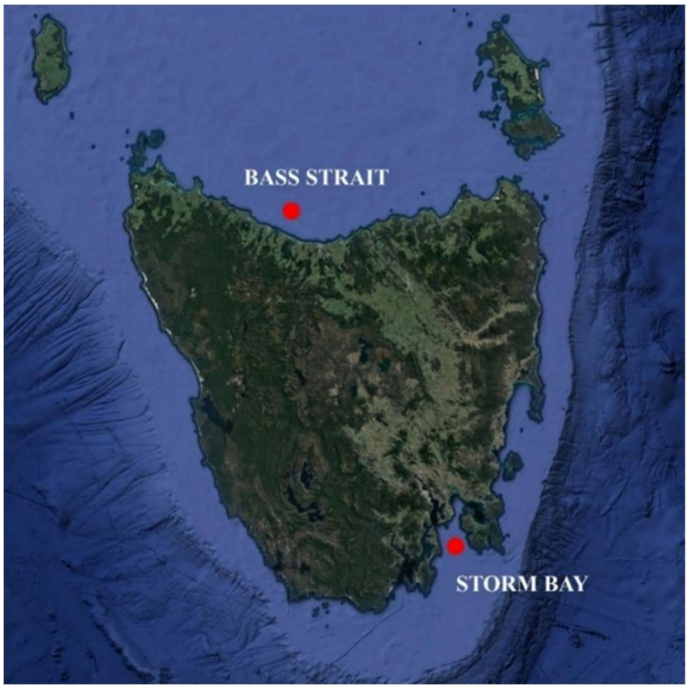


Figure 4. Selected locations for the case study of offshore Tasmanian Atlantic salmon grow-out facilities. Red dots depict the coordinates of hypothetical farms, Bass Strait, and Storm Bay.

The Bass Strait and Storm Bay sites lie in nominal water depths of approximately 60 m and 130 m, respectively. Both are within the range served by floating, moored platforms rather than fixed foundations, consistent with the Saitec Offshore Technologies Swing-Around-Twin-Hull (SATH), pontoon-type, and

barge floaters adopted for the infrastructures evaluated here (Table 3). Water depth is used here to characterise the case study sites; it is not applied as a screening constraint within the influence diagram.

The case study represents an offshore Tasmanian Atlantic salmon grow-out facility with power demand profiles from [17], derived from European offshore operations observations [40,41]. The demand represents 2500 Head-on-Gutted tonnes annually (approximately 500,000 salmon), with 24-h profiles exhibiting on-peak and off-peak variations based on southern hemisphere operations. Monthly variations reflect production cycle phases. While actual facility demand fluctuates from these estimations, probabilistic analysis captures this variability through the Aquaculture Demand chance node.

Markov chain state thresholds correspond to on-peak and off-peak demands (Table 2, Figure 5), with state 8 unbounded above to capture generation exceeding 120 kWh. Further demand profile development details are available in [17].

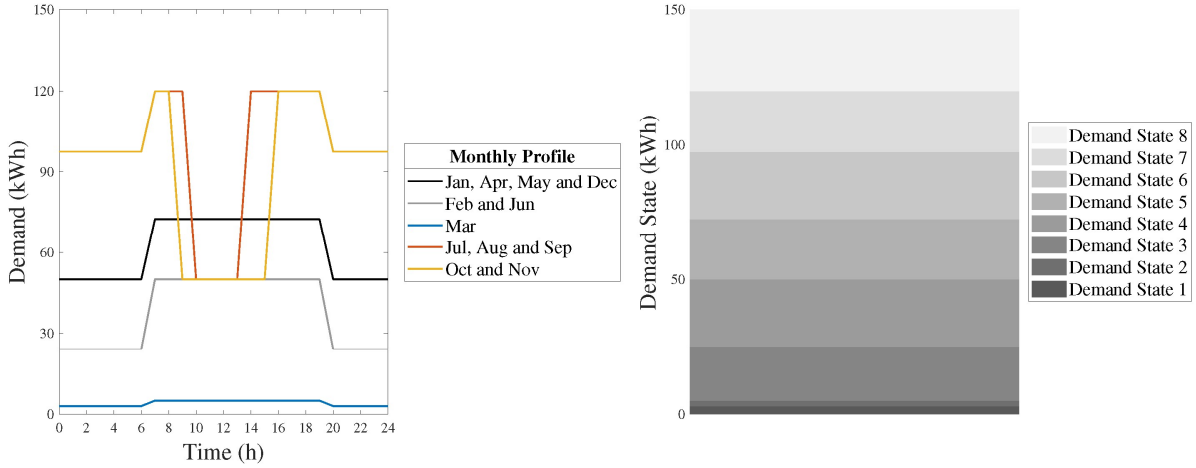


Figure 5. Aquaculture daily demand profiles (**left**) and time homogeneous demand states (**right**).

4.1. Power Generating Infrastructures

Six alternative infrastructures show the numerical decision-making model's application: five renewable energy configurations and one diesel generator baseline representing current practice (Table 3). Renewable infrastructures compare single-source versus multi-source solution effectiveness.

Preliminary sizing employed rated capacity and platform area metrics to maintain cross-concept comparability, thereby limiting utility amplification due to scale differences. Required capacity estimation utilised a demonstration project where 100 kW WEC capacity powered a 10,000 m^2 offshore aquaculture cage [42]. Scaling from the demonstration project's 15 fish/m^2 stocking density to the case study's production requirements yielded a 330 kW rated capacity target. While HAWT deployment at this scale is unlikely, infrastructure optimisation represents future work focus.

Table 3. Technical parameters of the alternative floating renewable energy infrastructure models relevant to the case study.

Technology	Device	Scale	Floater	Length (m)	Width (m)	Rated Capacity (kW)
HAWT	Suzlon S.33	350 kW	Saitec SATH	64	30	350
PV	CMP22270S	1630 m^2	Pontoon-type	64	30	325
HAWT PV	Aeolos-H60 CMP22270S	60 kW 1340 m^2	Saitec SATH	64	30	330
VAWT PV OWC	Aeolos-V10 CMP22270S N/A	8 × 10 kW 1340 m^2 50 m array	Barge Platform	50	30	320
PV OWC	CMP22270S N/A	1530 m^2 60 m array	Pontoon-Type	60	30	323

Multi-source platform energy shares were determined iteratively to maintain comparable topside areas (Figure 6). HAWT infrastructures employ SATH floaters, which weathervane around single-point moorings, eliminating wind directionality limitations. Maximum solar coverage is 85% of the platform topside, accommodating energy management and storage systems. Three multi-source configurations combine PV, wind turbines, and OWCs. Multi-source technologies diversify renewable resources, ideally reducing intermittency implications, though efficiency and scale of individual technologies decrease, reducing high instantaneous power instances.

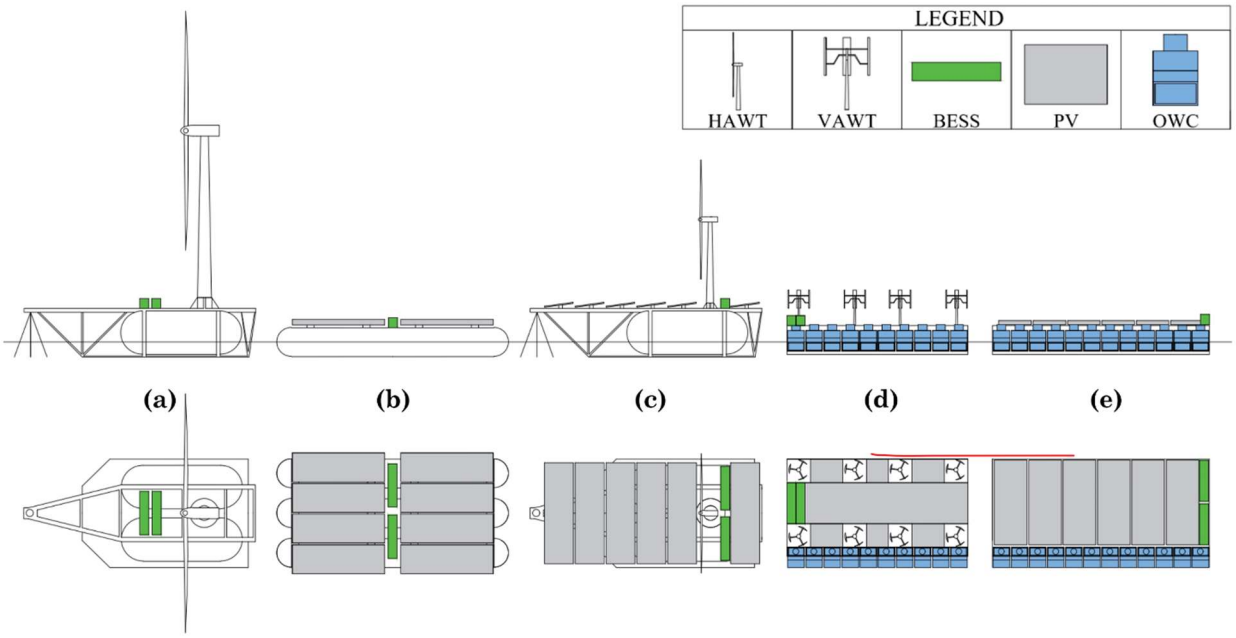


Figure 6. Block arrangement (profile and top view) of the five infrastructure concepts: (**a**) HAWT, (**b**) PV, (**c**) HAWT+PV, (**d**) VAWT+PV+OWC, (**e**) PV+OWC. Images not to scale.

The diesel generator (150 kW Caterpillar C7.1, operating at a constant 80% load) represents a traditional power solution with reduced capacity compared to renewable alternatives, since intermittency is absent. The five renewable alternatives are themselves diesel-renewable hybrids: diesel backup activates automatically whenever generation and storage are insufficient to meet demand, consistent with current industry practice for intermittent off-grid Power. The sixth alternative, diesel generation alone, represents the non-hybrid baseline against which the value of renewable adoption is measured, rather than an inconsistent point of comparison. All six alternatives are evaluated against the same performance, environmental, and economic criteria; diesel's advantage in reliability reflects its constant-load operating characteristic rather than asymmetric treatment in the framework.

4.2. Battery Energy Storage System

BESS mitigates renewable resource intermittency by storing surplus energy for deficit periods. Scalable lithium-ion systems were selected from available technologies [43]. The influence diagram decision node considers five capacity alternatives: 0, 500, 1000, 1500, and 2000 kWh. No separate rated charge/discharge power (kWh) limit is applied—the model assumes the battery's power electronics can absorb or release whatever hourly net differential occurs, up to the energy capacity limit itself. These capacities were selected through storage optimisation analysis balancing cost-performance trade-offs: preliminary temporal simulations identified that renewable infrastructures experienced power deficits ranging from 2–8 h duration depending on site and configuration, establishing a minimum viable capacity of around 500 kWh (sufficient for 4-h average deficit periods at mean demand levels). The 2000 kWh upper

bound was established where marginal utility gains diminished (capacity factors >80% were achieved) while costs escalated nonlinearly, representing the practical limit at which additional storage provides minimal performance improvement relative to the expense. The 500 kWh increments enable systematic evaluation of the storage-cost-performance relationship across this optimised range. Larger batteries extend renewable energy availability after resources decline below demand but incur proportionally higher costs, as captured in the COVE analysis. Excess electricity beyond BESS capacity may power auxiliary aquaculture operations (desalination, amenities, pumping, cleaning). Since these operations exceed the research scope, any excess energy beyond the maximum charge is considered dissipated. Excess energy also presents lithium-ion battery longevity and safety hazards [44], making performance utility dependent on Battery State chance nodes.

4.3. Resources

Wind direction effects on turbine performance were neglected: HAWT turbines utilise SATH hulls with omnidirectional capability, and VAWTs operate independent of wind direction. Wind turbine conversion efficiencies employ respective power curves. Temporal solar irradiation from NASA Data Access Viewer [45] used 'all sky' data accounting for weather-induced irradiation reduction. PV conversion efficiency is 23.7% (CMP22270S marine series), characteristic of commercial systems. Performance ratio is 75%, conservative for offshore PV [46], assuming optimised tilt angles and reduced shadow effects. The 150 kW Caterpillar C7.1 diesel generator operates at a constant 80% load, maximising output and fuel consumption [36].

COVE estimations are preliminary due to limited historical data for SATH floating wind, offshore PV, and OWCs required by [37]. Broader classifications—floating offshore wind turbines (FOWT), FPV, and WECs—substitute specific device data, justified by technology immaturity and limited public domain cost analyses. Where values are unavailable, parameters are equalised across infrastructures to avoid epistemic uncertainty bias. While this yields inaccurate absolute cost predictions, consistent assumptions produce comparative error between technologies. Table 4 presents the technology classification characteristics used in the annual investment cost calculation (Equation (6)).

The cost parameters in Table 4 are 2030 forecast values for the two Tasmanian case study sites. They are reported to demonstrate the COVE calculation and to support the sensitivity analysis of Section 5.4, and are not offered as a price forecast; comparative results elsewhere in this paper are expressed relative to the diesel baseline rather than in absolute terms.

Table 4. Characteristics of investment cost forecasting methodology for renewable energy technology classes used in case study.

Technology	Installed Capacity x (GW)	Annual TRL y (-)	Learning Rate a (-)	Initial Investment C_0^* ($/kW)
FOWT	9.9	1	−0.0801	11,500
FPV	6	1	−0.2732	25,000
WEC	3	1	−0.1823	9000

1. Installed capacity in 2030 forecasts sourced in [47–49] for FOWT, FPV and WEC, respectively.
2. TRL of all technologies by 2030 is assumed to be 1, given the current TRL and learning curves.
3. Saturation value, ramp rate, and location parameter have been equalised to those of onshore wind energy [37].
4. Learning rate of FOWTs and FPVs is assumed equivalent to that of equivalent onshore technology [37].
5. Initial investment cost of FOWT is estimated as 44% greater than the onshore wind [37,50].
6. Initial investment cost of FPV is estimated as 25% greater than the onshore PV [37,51].
7. Initial investment cost and learning rate of a typical OWC are derived from [52].

BESS costs add $220,000 per 500 kWh capacity (Energetech Solar lithium-ion systems). Diesel generator annual investment comprises initial capital ($107,000) plus annual fuel costs ($417,300 based on

2030 diesel price forecasts [53]). Valued energy determination iterates through temporal data for demand, battery charge, and generation. Demand-generation differences establish surplus or deficit for each timestep. Surplus timesteps yield valued energy fractions equal to demand. Deficit timesteps yield valued energy equal to demand (if battery charge suffices) or available battery power. This process estimates the actual Power utilised by aquaculture facilities, considering stochastic generation behaviour.

4.4. Decision Making

MAU theory application assumes potential future government initiatives promoting renewable energy in aquaculture. Tasmania demonstrates precedents through infrastructure subsidies contributing to carbon offset, notably the $2.5 million Energy on Farms Solar Project [54], supporting solar array installations for irrigation pump stations. Combined with the Tasmanian Salmon Industry Plan [6], this supports the assumption that the government may provide financial support for environmentally sustainable offshore aquaculture growth. This anticipated initiative impacts decision-making twofold: increasing environmental criterion weight and reducing economic criterion weight. Following the AHP pairwise comparison methodology [32], intensity assignments are shown in Table 5.

Table 5. Pairwise comparisons of the criteria following the AHP method.

Criteria A	Criteria B	More Important	Intensity
Performance	Environment	B	3
Environment	Economic	A	5
Economic	Performance	B	2

5. Results and Discussion

Figure 7 shows temporal power generation for four infrastructure models at the Bass Strait site, superimposed over aquaculture demand threshold states. Renewable energy technologies exhibit state transitions driven by resource intermittency, while diesel generation (Figure 7d) maintains constant output throughout the annual time history.

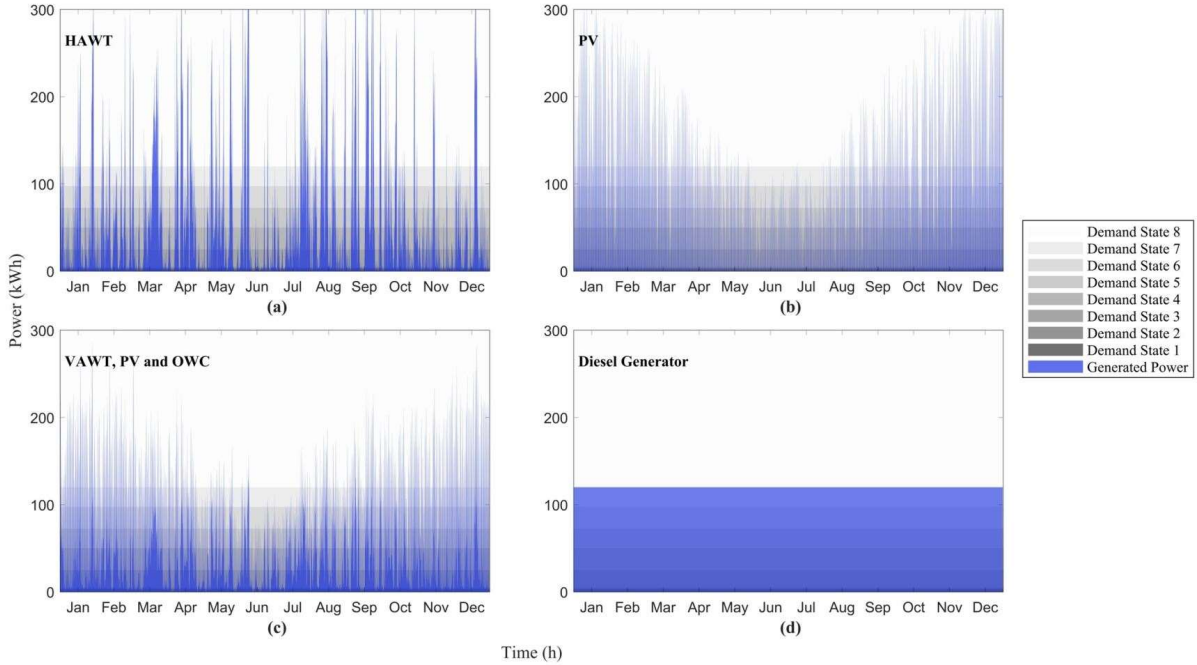


Figure 7. Yearly power generation of four key infrastructure models superimposed over aquaculture demand states. Generation profiles are indicative of the Bass Strait site for the (**a**) HAWT; (**b**) PV; (**c**) VAWT, PV and OWC; and (**d**) Diesel models.

The single-source wind turbine (Figure 7a) exhibits large stochastic peaks that frequently reach demand state 8, though power generation fluctuates across states for most of the year. Single-source PV (Figure 7b) exhibits clear diurnal intermittency with daily peaks returning to zero overnight. PV resource availability at Bass Strait shows seasonal variation: summer months provide higher generation suitable for peak aquaculture demands, while winter daily peaks fall below the highest demand state. This seasonal pattern aligns favourably with aquaculture demand fluctuations corresponding to the Atlantic Salmon growth cycle (Figure 5). Multi-source infrastructures (Figure 7c) mitigate solar intermittency by providing baseline wind or wave generation during off-peak periods, consistent with findings in [17].

State transitions are central to the Markov chain methodology employed in this study. Figure 8 presents a detailed view of transitions for the multi-source infrastructure, counted at hourly time-step intervals and presented in the transition probability matrix (Table 6). The matrix shows that the demand state occupied by power generation remains constant (λ_{nn}) between consecutive intervals more frequenty than not, and that generation concentrates in the lower-bound (State 1) and upper-bound (State 8) states—the defining states for the performance utility ranking.

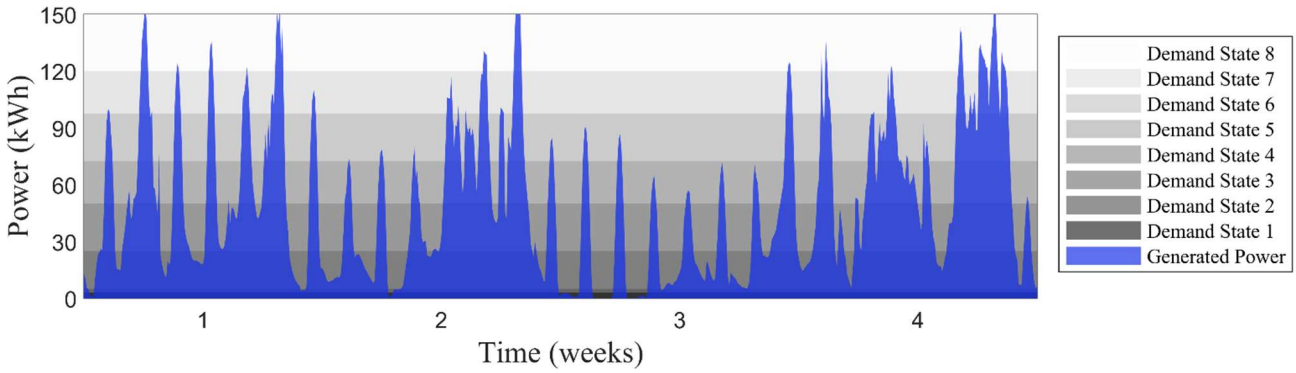


Figure 8. Monthly (April) power generation of VAWT, PV, and OWC multi-source infrastructure in the Bass Strait superimposed over aquaculture demand states. Transitions between states can be observed in high fidelity.

Table 6. Transition matrix and stationary distribution of multi-source VAWT, PV, and OWC infrastructure in the Bass Strait.

	State 1	State 2	State 3	State 4	State 5	State 6	State 7	State 8	Stationary Distribution
State 1	0.83	0.08	0.07	0.00	0.00	0.00	0.00	0.00	0.072
State 2	0.14	0.54	0.28	0.01	0.00	0.00	0.00	0.00	0.038
State 3	0.02	0.05	0.76	0.13	0.02	0.00	0.00	0.00	0.208
State 4	0.00	0.00	0.17	0.58	0.19	0.04	0.00	0.00	0.174
State 5	0.00	0.00	0.02	0.27	0.42	0.21	0.05	0.00	0.132
State 6	0.00	0.00	0.00	0.06	0.27	0.38	0.20	0.06	0.114
State 7	0.00	0.00	0.00	0.00	0.08	0.29	0.32	0.28	0.078
State 8	0.00	0.00	0.00	0.00	0.00	0.05	0.11	0.83	0.183

The relationship between energy storage capacity and economic performance is illustrated in Figure 9. Multi-source infrastructures exhibit decreasing COVE with increased battery capacity, indicating improved economic value. Conversely, single-source infrastructures show increasing COVE with larger batteries, suggesting diminishing economic returns. This divergence reflects the ability of multi-source systems to better utilise stored energy by maintaining more consistent generation profiles, thereby reducing the proportion of unused capacity. Diesel generation is excluded from Figure 9 as it requires no battery storage; its COVE establishes the baseline against which renewable energy infrastructures are compared. The economic advantage of larger batteries for multi-source systems also corresponds to reduced diesel generator runtime, thereby decreasing environmental impact as demonstrated in [17].

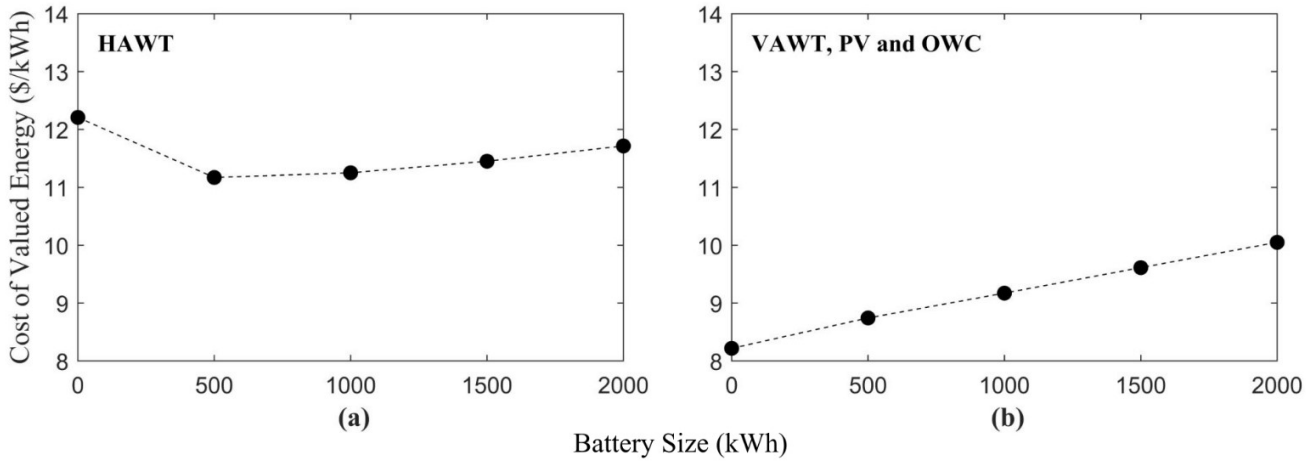


Figure 9. COVE versus battery capacity for HAWT (**a**) and VAWT+PV+OWC (**b**) infrastructures.

5.1. Additive Linear Utility

Expected ALU values for all six alternatives at both sites, computed by the influence diagram under equal criterion weighting, are presented in Figure 10.

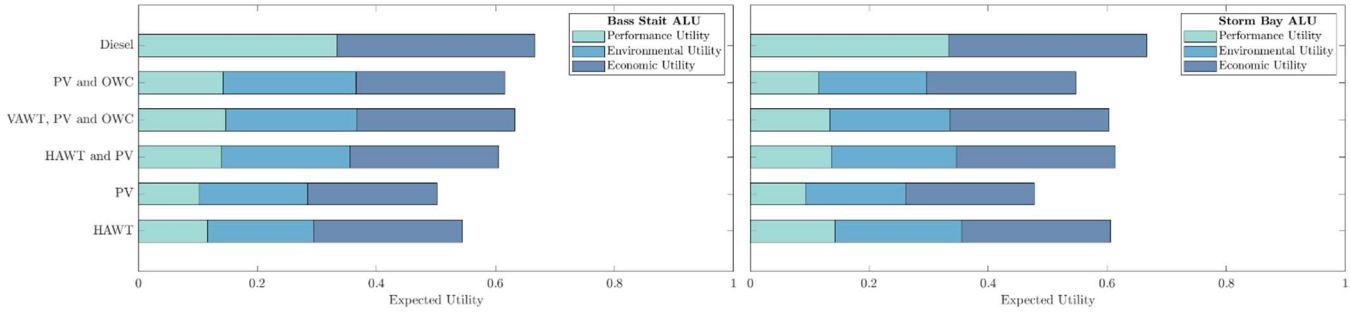


Figure 10. Expected utilities by infrastructure (ALU) at Bass Strait (**left**) and Storm Bay (**right**); bar segments show the performance, environmental, and economic components of each total.

Renewable energy infrastructure designs at both Bass Strait and Storm Bay did not achieve utilities comparable to diesel generation under the selected assessment criteria. This disparity stems primarily from resource intermittency, which adversely affects both performance and economic criteria by reducing capacity factors and increasing COVE values. Utilities for identical designs vary between the two sites, indicating that resource availability substantially influences system performance. Environmental and performance utilities are coupled: infrastructures achieving higher technical performance also achieve better environmental performance through reduced diesel generator reliance.

The optimal renewable infrastructure differs between sites: Bass Strait favours the VAWT-PV-OWC combination, while Storm Bay achieves maximum utility with the HAWT-PV system. This finding directly addresses the primary research objective, showing that no universally deployable solution exists across the case study sites. Rather, site-specific renewable energy configurations are necessary to maximise utility, reflecting the influence of location-dependent resource characteristics on infrastructure performance.

5.2. Multi-Attribute Utility

MAU analysis shows how decision-maker preferences affect infrastructure rankings within the influence diagram framework. The MAU approach reflects real-world scenarios in which objectives have varying importance to stakeholders. Following the case study scenario, criterion weightings were

established as 23.0% for performance, 64.8% for environmental impact, and 12.2% for economic feasibility, derived through AHP pairwise comparisons.

MAU weighting alters infrastructure rankings compared to the ALU approach (Figure 10), as shown in Figure 11 and Table 7. At Bass Strait, the VAWT-PV-OWC multi-source platform achieves highest utility, while Storm Bay favours the HAWT-PV system. Notably, renewable infrastructures rank higher than diesel generation under MAU weighting that prioritises environmental performance over economic criteria. This outcome aligns with current policy drivers, including fossil fuel reduction mandates and international commitments such as the Paris Agreement. The results suggest that economic incentives or subsidies reducing renewable technology costs could enhance the viability of offshore renewable energy for off-grid applications by improving their economic utility component.

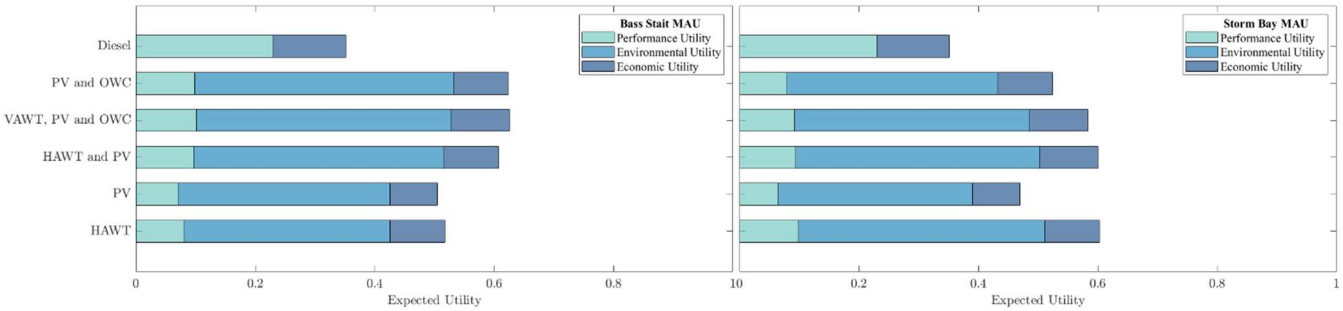


Figure 11. Expected utilities by infrastructure (MAU; weights 23% performance, 64.8% environmental, 12.2% economic) at Bass Strait (**left**) and Storm Bay (**right**).

The MAU framework extends the model's applicability by accommodating stakeholder-specific weightings that reflect varying social, policy, and economic priorities. While the case study weightings are assumption-based, they exhibit the methodology's flexibility for real-world application. The MAU results are consistent with the ALU findings in this respect.

Table 7. Top three MAU-ranked alternatives at each site, with diesel baseline for reference. COVE in $/kWh, with the ratio to the diesel baseline given alongside; diesel usage and curtailment as percentage of annual operating hours.

Site	Infra.	Batt. (kWh)	ALU	MAU	COVE ($/kWh)	Ratio to Diesel	Diesel (%)	Curt. (%)
Bass Strait	VAWT+PV+OWC	1500	0.633	0.625	9.61	10.4	25.5	19.8
	VAWT+PV+OWC	2000	0.619	0.624	10.05	10.9	24.9	19.2
	PV+OWC	1500	0.616	0.624	11.60	12.6	25.7	17.1
	Diesel	–	0.667	0.352	0.92	1	100	0
Storm Bay	HAWT+PV	2000	0.602	0.603	10.72	11.7	27.2	17.2
	HAWT	2000	0.605	0.603	10.25	11.1	31.0	25.3
	HAWT+PV	1000	0.614	0.601	9.87	10.7	28.9	18.7
	Diesel	–	0.667	0.352	0.92	1	100	0

To identify the specific threshold at which environmental weighting reverses the diesel-favouring ALU ranking, criterion weights were interpolated linearly between the equal weighting and the AHP-derived (23.0%/64.8%/12.2%), and the resulting MAU ranking recalculated at each interpolation step. Renewable infrastructures overtake diesel generation once the environmental weight reaches approximately 36.8% at Bass Strait and 38.9% at Storm Bay—both well short of the full AHP-derived weighting, indicating the ranking reversal is not an artefact of the particular weights adopted here, but occurs across a broad range of plausible stakeholder priorities between the two scenarios already reported.

5.3. TOPSIS Benchmark Comparison

To address the reliance on a single decision-making method, the ALU and MAU rankings were benchmarked against the TOPSIS [55], applied independently to each site using the same three decision criteria and the same two weighting schemes (equal weighting and the AHP-derived weighting of Table 5). Table 8 summarises the top-ranked renewable configuration identified by each method.

TOPSIS independently corroborates the Bass Strait finding under both weighting schemes, identifying the same VAWT-PV-OWC multi-source configuration as optimal. At Storm Bay, however, TOPSIS identifies a different top-ranked configuration under one weighting scheme. This divergence is attributed primarily to differences in normalisation methodology: ALU/MAU utilities are min-max normalised relative to the range of alternatives evaluated (Section 2.5), whereas TOPSIS applies vector normalisation to each criterion independently, which can weight close-ranked alternatives differently when relative magnitudes are similar. The Storm Bay rankings across the top several alternatives are comparatively close, which plausibly makes the ranking more sensitive to this methodological choice than Bass Strait's more clearly separated alternatives.

Table 8. Comparison of the top-ranked renewable infrastructure identified by ALU/MAU versus TOPSIS, by site and weighting scheme.

Site	Weighting	ALU/MAU-Optimal	TOPSIS-Optimal
Bass Strait	Equal (ALU-parallel)	VAWT-PV-OWC	VAWT-PV-OWC
Bass Strait	AHP (MAU-parallel)	VAWT-PV-OWC	VAWT-PV-OWC
Storm Bay	Equal (ALU-parallel)	HAWT-PV	VAWT-PV-OWC
Storm Bay	AHP (MAU-parallel)	HAWT-PV	HAWT-PV

5.4. Economic Assessment and Cost Sensitivity

The economic model (Section 2.3) relies on forecast cost parameters—initial investment cost, technology learning rate, and installed capacity projections for 2030—that are inherently uncertain for the low-maturity technologies evaluated here. To assess how this uncertainty propagates through to COVE and the resulting infrastructure ranking, a one-at-a-time sensitivity analysis was conducted, independently perturbing each parameter by ±20% for each of the three technology classes underlying the investment-cost model (floating offshore wind, FPV, and WEC/OWC; Table 4). All absolute cost figures reported in this section are 2030 forecast values specific to the two case study sites; the comparative findings that follow are expressed as relative changes and are independent of the absolute price level.

The resulting change in COVE is summarised in Table 9, averaged across all evaluated infrastructure and storage-capacity alternatives. Initial investment cost was consistently the most influential parameter for every technology class, with FPV cost assumptions producing the largest effect (mean ±10.3% change in COVE across all alternatives, up to ±17.1% for PV-dominant configurations), followed by floating offshore wind (±4.9–5.3%) and WEC/OWC, which was consistently the least sensitive parameter tested (under ±3% in all cases).

Table 9. Mean percentage change in COVE across all alternatives under ±20% perturbation of each cost parameter, by technology class.

Technology	Initial Investment	Learning Rate	Capacity Forecast
FPV	±10.3%	±5.0–8.8%	±2.5–5.4%
Floating Offshore Wind	±4.9–5.3%	±0.9%	±0.4%
WEC/OWC	±0.7–1.0%	±0.2%	±0.15%

Despite these COVE variations, the resulting infrastructure ranking proved robust: re-evaluating the TOPSIS benchmark under each of the 36 perturbation scenarios (18 per site) did not change the top-ranked infrastructure at either site under either weighting scheme in 34 of 36 cases. In the remaining two cases—both under the largest single perturbation tested (FPV initial investment cost, +20%)—only the selected battery storage capacity within the already-optimal infrastructure shifted by one increment; the optimal infrastructure choice itself was unchanged.

Three further parameters raised in review—diesel price, battery cost, and TRL—were tested using the same approach. A ±20% diesel price perturbation changed the diesel baseline's COVE by ±15.5%; a ±20% battery cost perturbation ($220,000 per 500 kWh increment) changed renewable COVE by up to ±4.2% (mean ±1.8%); and a −20% reduction in assumed TRL (representing slower-than-assumed technology maturation) changed COVE by under 0.1% for all three technology classes, indicating the cost forecast is effectively insensitive to the TRL assumption within this model. Re-evaluating the TOPSIS benchmark under these 28 further scenarios again left the optimal infrastructure unchanged in all cases, with only two further battery-capacity-level shifts (both under battery cost perturbation). Across all six cost parameters tested (64 scenarios in total), the optimal infrastructure choice at each site was unchanged in every case, indicating that while absolute COVE values are sensitive to cost-forecast uncertainty as expected for low-maturity technologies, the comparative infrastructure ranking underlying this study's conclusions is robust to that uncertainty within the ranges tested.

5.5. Implications

The numerical results yield valuable implications across industry practice, methodology, and policy domains. For industry stakeholders, the findings demonstrate that, across the two resource profiles examined in this study, universal "one-size-fits-all" deployment strategies did not produce the highest-utility outcome at both sites; this suggests such strategies warrant caution more broadly across offshore aquaculture renewable energy systems, though confirming this beyond the tested conditions would require additional site assessments. Multi-source infrastructures exhibit improved economic performance with increased battery capacity, in contrast to single-source systems, where larger batteries diminish economic value, indicating that energy storage optimisation must consider infrastructure type and the complementarity of generation profiles.

These results relate to two previously cited studies. Villalba et al. [7] evaluated 36 offshore-wind-only alternatives (foundation type, site selection, aquaculture species pairing) across three Tasmanian sites, identifying a single robust optimum within that technology; as their study did not compare across energy source types, it addresses a different question to the present finding that no single source or combination generalises across sites, and the two results are complementary rather than conflicting. This finding also reinforces the rationale for adopting COVE over LCOE [26], since a single-metric techno-economic comparison would similarly fail to capture the site-dependent trade-offs shown here.

Methodologically, the probabilistic decision-making framework successfully integrates temporal uncertainty through Markov modelling, economic forecasting via investment cost projections, and multi-criteria evaluation through influence diagrams. This approach is transferable to other off-grid renewable energy applications beyond aquaculture, where site-specific assessment under uncertainty is required. The MAU sensitivity analysis reveals that renewable infrastructures become competitive with diesel generation when environmental objectives are appropriately weighted, reflecting commitments such as the Paris Agreement. This finding suggests that policy interventions—including subsidies, carbon pricing mechanisms, or renewable energy mandates—could accelerate offshore renewable energy adoption by aligning economic incentives with environmental performance objectives, thereby bridging the current competitiveness gap identified under equal criterion weighting.

For offshore operators or consultants considering practical application of this framework, three categories of input data are required: (i) site-specific temporal resource data (wind, solar, and wave), obtainable from open-access sources such as the NASA POWER Data Access Viewer and national bathymetric/marine mapping services, ideally validated against local meteorological observations as in Section 4; (ii) an aquaculture power demand profile, either from operational records for an existing facility or estimated from production targets as done here; and (iii) technology cost data, which may be sourced from vendor quotations where available or from published cost-forecasting literature as in Table 4 where they are not. Computationally, the temporal simulation and probabilistic evaluation (Appendix A) run on standard desktop computing hardware within a MATLAB environment, with the resulting probabilities populating an influence diagram evaluated in GeNIe; neither step requires high-performance computing resources. The implementation workflow follows Appendix A directly: resource and demand data acquisition, temporal power generation and DTMC modelling, COVE calculation, influence diagram population, stakeholder-weight elicitation via AHP, and MAU-based ranking of alternatives. In practice, the primary driver of implementation timeline is likely to be data acquisition and stakeholder weight elicitation rather than computation itself, since the latter completes in a comparatively short period once input data are assembled; we do not report a specific timeline estimate, as this would depend heavily on data availability and stakeholder engagement processes specific to each project.

5.6. Future Works

The site-dependent optimal infrastructure configurations (Figures 10 and 11) indicate substantial potential for framework expansion. Results from [17] and this study suggest modular, scalable powering systems offer promising approaches for off-grid aquaculture. Model robustness could be enhanced by incorporating additional site characteristics, including port accessibility, industrial zoning constraints, and water depth limitations, as demonstrated in [27]. Probabilistic modelling improvements should consider larger temporal datasets and additional performance-affecting phenomena such as wave breaking, turbine stalling, and PV tilt angle optimisation.

While beyond the current study's scope, platform engineering feasibility represents a critical area for future investigation. Detailed structural analysis should address expected operational lifetime under marine conditions, extreme weather survivability (storm loading, wave impact, corrosion), and mooring system reliability to establish realistic deployment constraints. Integrating these engineering considerations would improve the framework's practical applicability by ensuring that infrastructure recommendations are technically viable.

Similarly, environmental permitting and marine spatial planning considerations, though outside the scope of this study, are essential for real-world deployment. Future research should incorporate regulatory frameworks, ecological impact assessments, marine protected area restrictions, shipping lane conflicts, and stakeholder consultation requirements into the decision-making model, as site access depends heavily on these constraints.

The preference for multi-source infrastructures suggests energy share optimisation warrants investigation. Infrastructure optimisation using established criteria could yield modular designs where configuration adapts to site-specific resources. While MAU sensitivity was preliminarily assessed, findings indicate stakeholder-weighted criteria may be essential for industry adoption. Effective implementation requires industry expert collaboration to quantify weightings [29], employing systematic bias-equalisation methods [56] to maintain objectivity while accommodating legitimate stakeholder preferences.

The probabilistic decision-making methodology developed here is also applicable beyond the planning stage addressed in this study: the same influence-diagram and Markov-chain structure could underpin digital twin environments, AI-assisted real-time decision support, and continuous condition monitoring

within broader offshore energy management systems, extending its use from static infrastructure selection toward dynamic, in-operation decision-making.

5.7. Scope and Limitations

The framework presented in this study addresses the selection of renewable energy infrastructure under resource and demand uncertainty; it is not a structural or marine-engineering design methodology. Accordingly, structural integrity, hydrodynamic response, structural survivability under extreme sea states, mooring system reliability, fatigue loading, corrosion, and maintenance accessibility are outside the scope of the influence-diagram framework and are not incorporated into the reported utility rankings. These factors are acknowledged as necessary complementary analyses for any candidate infrastructure prior to deployment, and are identified as priorities for future integration rather than omissions from the present framework's intended scope.

Similarly, the two-site Tasmanian case study demonstrates the framework's application and enables a comparative evaluation of the influence of site-specific resources on infrastructure ranking; it does not constitute a statistically representative sample of offshore aquaculture sites globally. The conclusion that no universally optimal configuration exists should accordingly be read as evidence against a one-size-fits-all deployment strategy under the tested conditions, rather than a general claim that extends beyond the resource and demand characteristics examined here.

The economic assessment likewise remains preliminary: it captures capital investment cost normalised by valued energy delivered, but does not yet incorporate operational and maintenance costs, replacement costs, component degradation, or offshore accessibility & diesel fuel logistics, each of which may materially affect absolute (though not necessarily comparative) cost outcomes.

Validation of the framework against measured operational data was not possible, as no offshore aquaculture installation currently operates at this scale on renewable Power—a gap this framework is intended to help address, rather than a validation source it can draw on. The evidence available in its place is the goodness-of-fit check completed in Section 2.4, in which the fitted transition matrices reproduce the empirical state-occupancy distributions of the underlying generation series to within a total variation distance of 0.0033 across all infrastructures at both sites; qualitative consistency with the independent findings of Roberts et al. [17] regarding multi-source mitigation of solar intermittency; the criterion-weight sensitivity analysis already reported; and a TOPSIS benchmark comparison (Section 5.3) conducted against the ALU/MAU rankings at both sites. That comparison corroborates the Bass Strait ranking under both weighting schemes, but identifies a different top-ranked configuration at Storm Bay, indicating that the site-specific rankings reported here are, at least at Storm Bay, sensitive to the choice of multi-criteria method. Operational validation against measured data remains a priority direction for future work as suitable installations become available, as does benchmarking against further MCDM methods (e.g., VIKOR, PROMETHEE, ELECTRE) beyond the TOPSIS comparison undertaken here.

Parameter sensitivity has been assessed for both the economic model (Section 5.4) and the criterion weighting, and neither was found to change the qualitative site-specific conclusions within the ranges tested. However, full uncertainty propagation through the framework—e.g., Monte Carlo resampling of the underlying resource and demand time series to generate confidence intervals or uncertainty bands around the reported expected utility values, rather than single point estimates—was not undertaken, and is identified as a substantial priority extension for future work rather than a component of the present analysis.

6. Conclusions

This research developed a probabilistic decision-making framework that integrates influence diagrams, Markov chains, and multi-attribute utility theory to evaluate renewable energy infrastructure for offshore aquaculture based on performance, environmental, and economic criteria.

Applied to two Tasmanian sites assessing six alternatives, the framework identified different optimal configurations at each site—Bass Strait favoured VAWT-PV-OWC while Storm Bay achieved maximum utility with HAWT-PV—indicating that, for the two resource profiles and demand conditions examined, site-specific resource characteristics rather than universal standardization determined optimal solution. Multi-source infrastructures outperformed single-source alternatives at both sites, reflecting the complementarity of wind, solar, and wave resources in reducing intermittency. These ranking proved insensitive to the cost assumptions underpinning them: across all 64 cost-parameter perturbation scenarios tested (±20% on six parameters), the top-ranked infrastructure at each site was unchanged in every case.

The competitiveness of renewable infrastructure against diesel generation proved contingent on criterion weighting rather than on cost level. Under equal weighting, renewable energy alternatives scored 15–35% lower in utility, at a COVE approximately 9–14 times the diesel baseline on a 2030 forecast basis. This ranking reversed once the environmental criterion weighting exceeded 36.8% at Bass Strait and 38.9% at Storm Bay, well short of the AHP-derived weighting of 64.8% adopted in this case study.This threshold is unaffected by subsequent movement in either renewable or diesel prices, and locates the point at which stakeholder priorities rather than technology costs govern the outcome.

Confirming site-specificity as a general principle for offshore aquaculture power would require extension to additional sites and multi-year resource data, which we identify as a priority direction for future work, alongside infrastructure optimisation and refinement of the energy storage representation. For policymakers, the weighting threshold indicates the scale of environmental valuation—whether expressed through incentives, carbon pricing, or procurement criteria—at which renewable infrastucutre becomes the preferred option on these criteria. Offshore developers and aquaculture operators can apply the framework for site-specific assessments incorporating local resource data, stakeholder priorities through systematic MAU weighting, and constraints including port accessibility and water depth.

Supplementary Materials

The following supporting information can be found at: https://www.sciepublish.com/article/pii/1245, File S1: GeNIe network file.

Appendix A. Numerical Model Workflow

Algorithm A1: Numerical Model Computational Sequence

1. **Input:** Site resources (wind, solar, wave), infrastructure specifications, battery capacities, demand profiles

2. For each infrastructure i:

   a. Calculate temporal power generation: $P_{PV}(t)$, $P_{wind}(t)$, $P_{wave}(t)$
   b. Compute combined power: $P_{combined}(t) = P_{PV}(t) + P_{wind}(t) + P_{wave}(t)$
   c. Build DTMC transition matrix from $P_{combined}(t)$
   d. Calculate stationary distribution (eigenvector)
   e. For each battery capacity b:
      i. Model battery state of charge over time history
      ii. Determine state of system probability: $P(sufficient|i,b)$
      iii. Calculate battery status: $P(charged|sufficient,i,b)$, $P(overcharged|sufficient,i,b)$
      iv. Compute valued energy and COVE

3. Populate influence diagram chance nodes with computed probabilities
4. Evaluate utility functions for each criterion
5. Calculate expected utilities: ALU or MAU with AHP-derived weights
6. **Output:** Ranked infrastructure alternatives with utilities

Statement of the Use of Generative AI and AI-Assisted Technologies in the Writing Process

During the preparation of this manuscript, the author(s) used Anthropic's Claude Sonnet 5 for grammatical revision and language editing. After using this tool/service, the author(s) reviewed and edited the content as needed and take full responsibility for the content of the published article.

Acknowledgments

The authors acknowledge the support of the Blue Economy Cooperative Research Centre and the Australian Maritime College.

Author Contributions

Conceptualization, D.H. and T.V.; Methodology, T.V. and D.H.; Software, T.V.; Validation, T.V. and D.H.; Formal Analysis, T.V.; Investigation, T.V.; Resources, T.V.; Data Curation, T.V.; Writing—Original Draft Preparation, T.V.; Writing—Review & Editing, D.H.; Visualization, T.V.; Supervision, D.H.; Project Administration, D.H.; Funding Acquisition, D.H.

Ethics Statement

Not applicable.

Informed Consent Statement

Not applicable.

Data Availability Statement

The data presented in this study are available from the corresponding author upon reasonable request.

Funding

The authors acknowledge the financial support of the Blue Economy Cooperative Research Centre, established and supported under the Australian Government's Cooperative Research Centres Program, grant number CRCXX000001 (previously 20180101). The article processing charge (APC) was waived by the publisher.

Declaration of Competing Interest

The authors declare that they have no known competing financial interests or personal relationships that could have appeared to influence the work reported in this paper.

References

1. The Business Research Company. *Aquaculture Global Market Report 2023*; The Business Research Company: Hyderabad, India, 2023.
2. Morro B, Davidson K, Adams TP, Falconer L, Holloway M, Dale A, et al. Offshore aquaculture of finfish: Big expectations at sea. *Rev. Aquac.* **2022**, *14*, 791–815. DOI:10.1111/raq.12625
3. Gentry RR, Lester SE, Kappel CV, White C, Bell TW, Stevens J, et al. Offshore aquaculture: Spatial planning principles for sustainable development. *Ecol. Evol.* **2017**, *7*, 733–743. DOI:10.1002/ece3.2637
4. Kaiser MJ, Snyder B, Yu Y. A review of the feasibility, costs, and benefits of platform-based open ocean aquaculture in the Gulf of Mexico. *Ocean Coast. Manag.* **2011**, *54*, 721–730. DOI:10.1016/j.ocecoaman.2011.07.005
5. AgriGrowth Tasmania. *Tasmanian Agri-Food ScoreCard 2020–21*; AgriGrowth Tasmania: Hobart, Australia, 2021.
6. Department of Natural Resources and Environment Tasmania. *Tasmanian Salmon Industry Plan 2023*; Department of Natural Resources and Environment Tasmania: Hobart, Australia, 2023.
7. Villalba J, Abdussamie N, Aryai V, Nikolova N, Tenekedjiev K, Wang C-M, et al. Assessment of uncertain alternatives for co-located aquaculture and offshore wind farm in Tasmania. *Ocean Eng.* **2022**, *249*, 110949. DOI:10.1016/j.oceaneng.2022.110949
8. Nieradzinska K, MacIver C, Gill S, Agnew G, Anaya-Lara O, Bell K. Optioneering analysis for connecting Dogger Bank offshore wind farms to the GB electricity network. *Renew. Energy* **2016**, *91*, 120–129. DOI:10.1016/j.renene.2016.01.043
9. U.S. Department of Energy. *Offshore Marine Aquaculture*; U.S. Department of Energy: Washington, DC, USA, 2019.
10. Briggs C, Teske S, Langdon R, Hemer M, Howard P, Marsh P. *Offshore Wind: Prospects for Australia*; Blue Economy Cooperative Research Centre: Launceston, Australia, 2021.
11. Freeman M, Garavelli L, Wilson E, Hemer M, Abundo M, Travis L. *Offshore Aquaculture: A Market for Ocean Renewable Energy*; Report for Ocean Energy Systems (OES): Lisbon, Portugal, 2022.
12. Johari MK, Jalil M, Shariff MFM. Comparison of horizontal axis wind turbine (HAWT) and vertical axis wind turbine (VAWT). *Int. J. Eng. Technol.* **2018**, *7*, 74–80. DOI:10.14419/ijet.v7i4.13.21333
13. Claus R, López M. Key issues in the design of floating photovoltaic structures for the marine environment. *Renew. Sustain. Energy Rev.* **2022**, *164*, 112502. DOI:10.1016/j.rser.2022.112502
14. Watson S, Moro A, Reis V, Baniotopoulos C, Barth S, Bartoli G, et al. Future emerging technologies in the wind power sector: A European perspective. *Renew. Sustain. Energy Rev.* **2019**, *113*, 109270. DOI:10.1016/j.rser.2019.109270
15. Falcão AF, Henriques JC. Oscillating-water-column wave energy converters and air turbines: A review. *Renew. Energy* **2016**, *85*, 1391–1424. DOI:10.1016/j.renene.2015.07.086
16. Howe D, Nader J-R, Macfarlane G. Performance analysis of a floating breakwater integrated with multiple oscillating water column wave energy converters in regular and irregular seas. *Appl. Ocean Res.* **2020**, *99*, 102147. DOI:10.1016/j.apor.2020.102147
17. Roberts S, Howe D, Nader J-R. Performance feasibility of a multi-source offshore renewable energy platform for aquaculture. In Proceedings of the ASME 2023 42nd International Conference on Ocean, Offshore and Arctic Engineering, Melbourne, Australia, 11–16 June 2023; Volume 86922; p. V010T13A012.
18. Nguyen HP, Wang CM. Advances in offshore aquaculture and renewable energy production. *J. Mar. Sci. Eng.* **2024**, *12*, 1679. DOI:10.3390/jmse12091679
19. Liu DP, Heo T. Co-locating offshore renewables and aquaculture: Feasibility, site-selection, and O&M synergies—A state of the art review. *Front. Mar. Sci.* **2026**, *13*, 1739325. DOI:10.3389/fmars.2026.1739325
20. Bertrand M, Giannini G, Majidi AG, Senocq C, Rosa-Santos P, Clemente D. Wave energy conversion to decarbonize offshore aquaculture: Multi-level techno-economic analysis for a case study in Peniche, Portugal. *Energies* **2025**, *18*, 5934. DOI:10.3390/en18225934
21. Delbeke O, Bastianel G, Yurtseven K, Ergun H, Moschner JD, Driesen J. Hybrid offshore solar-wind farms: The potential of integrating floating photovoltaics with offshore wind. *Appl. Energy* **2026**, *410*, 127486. DOI:10.1016/j.apenergy.2026.127486
22. Bao M, Arzaghi E, Abaei MM, Abbassi R, Garaniya V, Abdussamie N, et al. Site selection for offshore renewable energy platforms: A multi-criteria decision-making approach. *Renew. Energy* **2024**, *229*, 120768. DOI:10.1016/j.renene.2024.120768
23. Mao Q, Guo M, Lv J, Chen J, Xie P, Li M. A multi-criteria group decision-making framework for investment assessment of offshore floating wind-solar-aquaculture project under probabilistic linguistic environment. *Environ. Sci. Pollut. Res.* **2023**, *30*, 40752–40782. DOI:10.1007/s11356-022-24786-9

24. Fang Z, Zhu C, Zhou T. A comprehensive benefit evaluation of offshore wind–fishery integration projects from a sustainable development perspective: evidence from China. *Sustainability* **2026**, *18*, 2367. DOI:10.3390/su18052367
25. Ng CY, Ong MC. Concept selection of hybrid wave–current energy systems using multi-criteria decision analysis. *J. Mar. Sci. Eng.* **2025**, *13*, 1903. DOI:10.3390/jmse13101903
26. Vanegas-Cantarero MM, Pennock S, Bloise-Thomaz T, Jeffrey H, Dickson MJ. Beyond LCOE: A multi-criteria evaluation framework for offshore renewable energy projects. *Renew. Sustain. Energy Rev.* **2022**, *161*, 112307. DOI:10.1016/j.rser.2022.112307
27. Abaei MM, Arzaghi E, Abbassi R, Garaniya V, Penesis I. Developing a novel risk-based methodology for multi-criteria decision making in marine renewable energy applications. *Renew. Energy* **2017**, *102*, 341–348. DOI:10.1016/j.renene.2016.10.054
28. Salvador CB, Arzaghi E, Yazdi M, Jahromi HA, Abbassi R. A multi-criteria decision-making framework for site selection of offshore wind farms in Australia. *Ocean Coast. Manag.* **2022**, *224*, 106196. DOI:10.1016/j.ocecoaman.2022.106196
29. Wimmler C, Hejazi G, Fernandes E, Moreira C, Connors S. Multi-criteria decision support methods for renewable energy systems on islands. *J. Clean Energy Technol.* **2015**, *3*, 185–195. DOI:10.7763/JOCET.2015.V3.193
30. Howard RA, Matheson JE. *The Principles and Applications of Decision Analysis*; Strategic Decisions Group: Palo Alto, CA, USA, 1984; pp. 719–762.
31. Arzaghi E, Abaei MM, Abbassi R, O'Reilly M, Garaniya V, Penesis I. A Markovian approach to power generation capacity assessment of floating wave energy converters. *Renew. Energy* **2020**, *146*, 2736–2743. DOI:10.1016/j.renene.2019.08.099
32. Saaty TL. How to make a decision: The analytic hierarchy process. *Eur. J. Oper. Res.* **1990**, *48*, 9–26. DOI:10.1016/0377-2217(90)90057-I
33. Friis-Hansen A. *Bayesian Networks as a Decision Support Tool in Marine Applications*; Department of Naval Architecture and Offshore Engineering, Technical University of Denmark: Kgs. Lyngby, Denmark, 2000.
34. Aldersey-Williams J, Rubert T. Levelised cost of energy—A theoretical justification and critical assessment. *Energy Policy* **2019**, *124*, 169–179. DOI:10.1016/j.enpol.2018.10.004
35. Abdin Z, Mérida W. Hybrid energy systems for off-grid power supply and hydrogen production based on renewable energy: A techno-economic analysis. *Energy Convers. Manag.* **2019**, *196*, 1068–1079. DOI:10.1016/j.enconman.2019.06.068
36. Simpson J, Loth E, Dykes K. Cost of valued energy for design of renewable energy systems. *Renew. Energy* **2020**, *153*, 290–300. DOI:10.1016/j.enconman.2019.06.068
37. Sun W, Xiao J, Hou J, Jin C, Nie Y. Investment cost forecasting for low carbon power system planning considering technical progress and scale effect. *IEEE Access* **2022**, *10*, 114153–114164. DOI:10.1109/ACCESS.2022.3218060
38. Keeney RL, Raiffa H. *Decisions with Multiple Objectives: Preferences and Value Trade-Offs*; Cambridge University Press: Cambridge, UK, 1993.
39. Montibeller G, von Winterfeldt D. Biases and debiasing in multi-criteria decision analysis. In Proceedings of the 2015 48th Hawaii International Conference on System Sciences, Kauai, HI, USA, 5–8 January 2015; pp. 1218–1226.
40. Syse HL. *Investigating Off-Grid Energy Solutions for the Salmon Farming Industry*; University of Strathclyde: Glasgow, UK, 2016.
41. Møller S. Reduction of CO_2 Emissions in the Salmon Farming Industry: The Potential for Energy Efficiency Measures and Electrification. Master's Thesis, NTNU, Trondheim, Norway, 2019.
42. OES. Alternative Markets for Ocean Energy. 2021. Available online: www.ocean-energy-systems.org (accessed on 12 August 2023).
43. Yang Y, Bremner S, Menictas C, Kay M. Battery energy storage system size determination in renewable energy systems: A review. *Renew. Sustain. Energy Rev.* **2018**, *91*, 109–125. DOI:10.1016/j.rser.2018.03.047
44. Rad MAV, Kasaeian A, Niu X, Zhang K, Mahian O. Excess electricity problem in off-grid hybrid renewable energy systems: A comprehensive review from challenges to prevalent solutions. *Renew. Energy* **2023**, 212, 538–560. DOI:10.1016/j.renene.2023.05.073
45. NASA. POWER Data Access Viewer. 2023. Available online: https://power.larc.nasa.gov/data-access-viewer/ (accessed on 27 May 2023).
46. Golroodbari SZ, Ayyad AW, van Sark W. Offshore floating photovoltaics system assessment in worldwide perspective. *Prog. Photovolt. Res. Appl.* **2023**, *31*, 1061–1077. DOI:10.1002/pip.3723
47. Fernandez L. Newly Installed Offshore Floating Wind Capacity Worldwide in 2021, with a Forecast Until 2031. 2023. Available online: https://www.statista.com/statistics/1368098/floating-offshore-wind-new-installed-capacity/ (accessed on 12 August 2023).
48. IRENA. *Fostering a Blue Economy: Offshore Renewable Energy*; IRENA: Masdar City, Abu Dhabi, 2020.

49. Wimalaratna YP, Hassan A, Afrouzi HN, Mehranzamir K, Ahmed J, Siddique BM, et al. Comprehensive review on the feasibility of developing wave energy as a renewable energy resource in Australia. *Clean. Energy Syst.* **2022**, *3*, 100021. DOI:10.1016/j.cles.2022.100021
50. Stehly T, Duffy P. *2021 Cost of Wind Energy Review*; National Renewable Energy Lab. (NREL): Golden, CO, USA, 2022.
51. Oliveira-Pinto S, Stokkermans J. Assessment of the potential of different floating solar technologies—Overview and analysis of different case studies. *Energy Convers. Manag.* **2020**, *211*, 112747. DOI:10.1016/j.enconman.2020.112747
52. Hayward J. *Wave Energy Cost Projections: A Report for Wave Swell Energy Limited*; CSIRO: Canberra, Australia, 2022.
53. Graham PW, Smart A. *Possible Futures: Scenario Modelling of Australian Alternative Transport Fuels to 2050*; Department of Resources, Energy and Tourism: Canberra, Australia, 2011.
54. Tasmanian Irrigation. Energy on Farms Solar Project Underway. 2022. Available online: https://tasmanianirrigation.com.au/news/2022/energy-on-farms-solar-project-underway (accessed on 22 May 2023).
55. Hwang CL, Yoon K. *Multiple Attribute Decision Making: Methods and Applications, A State-of-the-Art Survey*; Springer Science & Business Media: Berlin/Heidelberg, Germany, 2012.
56. Rezaei J, Arab A, Mehregan M. Equalizing bias in eliciting attribute weights in multiattribute decision-making: Experimental research. *J. Behav. Decis. Mak.* **2022**, *35*, e2262. DOI:10.1002/bdm.2262